



Cite this: *Phys. Chem. Chem. Phys.*,  
2016, **18**, 970

Received 6th November 2015,  
Accepted 30th November 2015

DOI: 10.1039/c5cp06792h

www.rsc.org/pccp

## Tuning excitability by alloying: the Rh(111)/Ni/ H<sub>2</sub> + O<sub>2</sub> system

T. Smolinsky, M. Homann and R. Imbihl\*

The dynamic behavior of the O<sub>2</sub> + H<sub>2</sub> reaction on a Rh(111) surface alloyed with Ni has been studied in the 10<sup>−5</sup> mbar range using photoemission electron microscopy (PEEM) as a spatial resolving method. For  $T = 773$  K and  $p(\text{O}_2) = 5 \times 10^{-5}$  mbar the bifurcation diagram has been mapped out as a function of the Ni coverage in a range of  $0 \text{ ML} \leq \theta_{\text{Ni}} \leq 1.3 \text{ ML}$ . A critical Ni coverage of  $\theta_{\text{Ni,crit}} = 0.13$  monolayers (ML) is required for excitability. In the excitable parameter range pulse trains and irregular chemical wave patterns are found. Whereas the propagation speed of the pulses exhibits no clear-cut dependence on the Ni coverage, the frequency of the local PEEM intensity oscillations increases linearly with Ni coverage in the range from  $\theta_{\text{Ni}} = 0.13 \text{ ML}$  to  $\theta_{\text{Ni}} = 1.3 \text{ ML}$ .

## Introduction

Bimetallic catalysts play a prominent role in heterogeneous catalysis because by mixing two metals one can obtain a catalytic performance superior to each of the individual constituents.<sup>1</sup> While the electronic and adsorption properties of bimetallic surfaces have been well studied, not much is known about the dynamic behavior of bimetallic catalysts under reaction conditions.<sup>2–5</sup> Segregation effects, dealloying and chemical transformations might occur and change the composition of the surface depending on the reaction conditions. Recently Lovis *et al.* showed that by alloying a Rh(111) surface with nickel the originally bistable reaction system Rh(111)/O<sub>2</sub> + H<sub>2</sub> became excitable/oscillatory displaying chemical waves and rate oscillations.<sup>6</sup> An excitation mechanism has been proposed based on the reversible segregation of Ni to the surface. That earlier study has been conducted with a fixed amount of Ni corresponding to  $\theta_{\text{Ni}} \approx 0.25$  monolayers (ML) deposited on the surface. Here we study systematically the dynamic behavior of the reaction system as we vary the amount of deposited Ni from zero to several monolayers. The results are summarized in a bifurcation diagram.

The dynamic behavior of the O<sub>2</sub> + H<sub>2</sub> reaction on Rh(111) has been studied in the 10<sup>−5</sup> and 10<sup>−4</sup> mbar range using photoemission electron microscopy (PEEM) but only bistability was found.<sup>7</sup> Rate oscillations and propagating pulses were detected in the O<sub>2</sub> + H<sub>2</sub> reaction on a Ni foil but these studies were conducted at atmospheric pressure.<sup>8–10</sup> The reaction is non-isothermal under these conditions as evidenced by temperature pulses propagating on a Ni ring.<sup>10</sup> The rate oscillations and the chemical waves in the reaction on Ni were usually

discussed in terms of an oxidation–reduction mechanism. In fact, NiO formation was detected but a detailed mechanism still needs to be established.

On the alloyed Rh(111)/Ni surface a precipitation of small NiO particles was observed under reaction conditions but, first of all, the formation of NiO seems to be bound to higher Ni coverages and, secondly, these small NiO particles were more or less inert on the time scale of a chemical wave (a few seconds).<sup>6</sup> The NiO particles were therefore considered to play a kind of spectator role in the excitation mechanism but on a larger time scale and/or at higher pressure they might as well act as a kind of dynamic Ni reservoir in the excitation mechanism. In this paper we do not address the question of the mechanism which remains to be experimentally clarified but we focus on systematically investigating the influence of the amount of deposited Ni on the dynamic behavior of the reaction system. The dependence of the system behavior on the Ni coverage will of course pose a critical challenge for any excitation mechanism proposed for this reaction system.

## Experimental section

All experiments are carried out in a standard Ultra-High-Vacuum (UHV) chamber with a base pressure of  $5 \times 10^{-10}$  mbar, a chamber volume of 80 L and an effective pumping rate of 100 L s<sup>−1</sup>. The chamber is equipped with a photoemission electron microscope (PEEM),<sup>11</sup> an Auger electron spectrometer (AES) and LEED (low energy electron diffraction).

In the PEEM experiments the sample is illuminated with a deuterium discharge lamp with a wavelength of  $\sim 160$  to 400 nm. The emitted photoelectrons are collected with the PEEM optics and imaged onto a phosphorous screen. PEEM images

Institut für Physikalische Chemie und Elektrochemie, Leibniz Universität Hannover,  
Callinstrasse 3a, D-30167 Hannover, Germany. E-mail: imbihl@pci.uni-hannover.de

primarily the local work function with a spatial resolution of about 1  $\mu\text{m}$ .

Gases of purity 5.6 and 5.0 (both Linde) are used for hydrogen and oxygen. The pressures given here have been corrected for the smaller ionization probability of  $\text{H}_2$  by multiplying the read-out of the ionization gauge by a factor of 2.

The Rh(111) sample (Mateck) of dimensions  $10 \times 10 \times 1 \text{ mm}^3$  could be heated resistively through two Ta wires attached to it and through electron beam bombardment. The temperature is measured using a chromel/alumel (K-type) thermocouple.

Cleaning of the rhodium sample is done by repeated cleaning cycles of argon ion sputtering (1 kV, 773 K,  $p(\text{Ar}) \sim 5 \times 10^{-5} \text{ mbar}$ ) followed by flashing the sample to  $\sim 1300 \text{ K}$ . Afterwards the sample is heated in oxygen (1023 K,  $2.0 \times 10^{-6} \text{ mbar}$ ) and again flashed to  $\sim 1300 \text{ K}$ .

Nickel is deposited on the surface by electron beam evaporation from a 2 mm nickel rod (Goodfellow, purity: 99.99%). Nickel is evaporated at a sample temperature of 673 K and at a partial pressure of oxygen of  $2.0 \times 10^{-6} \text{ mbar}$ . Calibration of the Ni coverage is achieved by taking the change in the slope of the Ni AES signal plotted vs. the deposition time as one monolayer.

## Results and discussion

Ni is deposited always on a freshly prepared surface which was sputtered in order to avoid any Ni remnants of preceding reaction experiments. The Ni coverage was determined from AES using the monolayer calibration for Ni on Rh(111). For constructing the bifurcation diagram always the Ni coverage as determined directly after deposition was used. During exposure to reaction conditions the amount of Ni detectable by AES typically decreases by about 50–60% presumably because some Ni dissolves in the bulk region of the Rh crystal. This behavior is illustrated in Fig. 1 for an initial Ni coverage  $\Theta_{\text{Ni}} = 0.73 \text{ ML}$ . After 1–2 hours of exposure the Ni signal is already close to its stationary value. As indicated in the plot by the red line keeping the crystal after Ni deposition in an oxygen atmosphere at  $5.0 \times 10^{-5} \text{ mbar}$  drastically reduces the loss of Ni due to diffusion but a decrease of the Ni concentration is not completely suppressed. The strong scatter of the data does not result from noise in the Auger spectra but reflects the sensitivity of the system to slight changes in the preparation conditions.

The boundaries of the parameter range for excitability are mapped out for a fixed temperature  $T = 773 \text{ K}$  and for a fixed partial pressure of oxygen  $p(\text{O}_2) = 5.0 \times 10^{-5} \text{ mbar}$ . The system is excitable also at much higher temperature; chemical waves are seen at around 1000 K. Towards lower temperatures it becomes more and more difficult to observe chemical waves. At 473 K no excitability is observed any more. This temperature range agrees with the observations of Wander *et al.* who found out that vertical intermixing of Ni deposited on Rh(111) requires temperatures above 600 K.<sup>12</sup> The experiments are conducted such that the state of the surface under reaction conditions is monitored using PEEM while the partial pressure of hydrogen is varied as a control parameter.

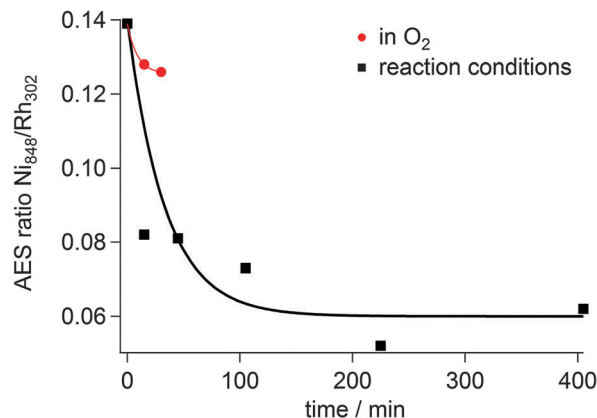
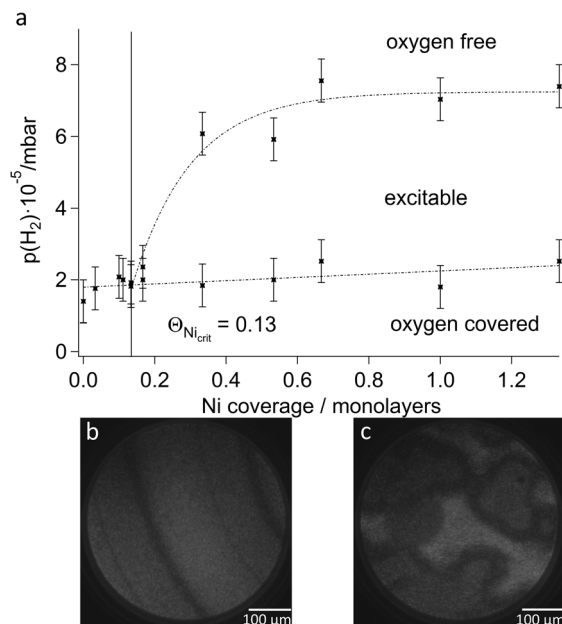


Fig. 1 Loss of Ni in the surface region under reaction conditions and in pure  $\text{O}_2$ . The ratio of the Ni signal at 848 eV to the Rh signal at 302 eV is plotted vs. time with  $t = 0$  referring to the completion of the Ni deposition for a coverage of  $\Theta_{\text{Ni}} = 0.73 \text{ ML}$  at  $T = 673 \text{ K}$  and  $p(\text{O}_2) = 2.0 \times 10^{-6} \text{ mbar}$ . The black bold line indicates the loss of the Ni signal under reaction conditions at  $T = 773 \text{ K}$ ,  $p(\text{O}_2) = 5.0 \times 10^{-5} \text{ mbar}$  and  $p(\text{H}_2) = 4.0 \times 10^{-5} \text{ mbar}$ . The red line marks the decrease of the Ni signal in pure  $\text{O}_2$  at  $T = 773 \text{ K}$  and  $p(\text{O}_2) = 5.0 \times 10^{-5} \text{ mbar}$ .

Upon variation of  $p(\text{H}_2)$  one obtains two limiting cases, an oxygen covered surface at low  $p(\text{H}_2)$  and a surface with a very low oxygen coverage at high  $p(\text{H}_2)$ . The excitability range is enclosed by these two boundaries. Depending on the direction in which  $p(\text{H}_2)$  is varied the boundaries differ by as much as 2% of  $p(\text{H}_2)$ .

For the bifurcation diagram the maximum and minimum values were taken so that the excitability range reaches its maximum extension. The bifurcation diagram one obtains in this way is displayed in Fig. 2a. The error bars in the diagram reflect the difficulty in determining visually the exact transition point and the scatter in the data when the experiment is repeated with a freshly prepared surface. The most remarkable feature in the bifurcation diagram is the existence of a critical Ni coverage  $\Theta_{\text{Ni,crit}} = 0.13 \text{ ML}$  which is required for the system in order to exhibit excitable behavior. Below this Ni coverage the system displays the bistable behavior of the clean Rh(111) surface with only small dependence of the boundary oxygen covered/oxygen free on the Ni coverage. A small hysteresis behavior could be observed here also but the values are quite close to each other (within 2%). In the diagram only the transition coming from an oxygen covered surface is indicated.

Mainly two kinds of pattern formation are observed. At the lower boundary, excitable/oxygen covered, one finds regular pulse trains in the excitability range originating from target patterns or spiral waves. A typical example of such a pulse train is displayed in Fig. 2b. In some cases, one also observes irregular wave patterns of the type displayed in Fig. 2c but within about 10 min the irregular waves transform into a regular pattern. Quite in contrast, at the upper boundary *i.e.* the boundary excitable/oxygen free one finds exclusively irregular pattern formation in the excitable range. These patterns remain irregular even after a long time under reaction conditions ( $> 4 \text{ hours}$ ).



**Fig. 2** (a) Bifurcation diagram for the  $\text{O}_2 + \text{H}_2$  reaction on a Rh(111) surface alloyed with varying coverages of Ni measured for  $T = 773 \text{ K}$  and with fixed  $p(\text{O}_2) = 5.0 \times 10^{-5} \text{ mbar}$ . The Ni coverage prior to exposure to reaction conditions was taken. The vertical line marks the critical Ni coverage  $\Theta_{\text{Ni,crit}} = 0.13 \text{ ML}$  necessary for obtaining excitable behavior. In the bistable range left of this line only the transition from the oxygen covered to the nearly oxygen free state of the surface is shown in the diagram. (b) PEEM image showing regular pattern formation at  $\Theta_{\text{Ni}} = 0.67 \text{ ML}$ ,  $p(\text{H}_2) = 4.0 \times 10^{-5} \text{ mbar}$ ,  $p(\text{O}_2) = 5.0 \times 10^{-5} \text{ mbar}$  and  $T = 773 \text{ K}$ . (c) PEEM image showing irregular pattern formation at  $T = 773 \text{ K}$ ,  $\Theta_{\text{Ni}} = 0.33 \text{ ML}$ ,  $p(\text{O}_2) = 5.0 \times 10^{-5} \text{ mbar}$  and  $p(\text{H}_2) = 5.0 \times 10^{-5} \text{ mbar}$ . For both PEEM images the field of view is  $500 \mu\text{m}$ .

In the system Rh(111)/ $\text{O}_2 + \text{H}_2$  the assignment of the grey levels in PEEM to adsorbates is simple. Chemisorbed oxygen appears as a dark area in PEEM due to the work function (WF) increase caused by the strongly electronegative oxygen; bright areas represent a nearly adsorbate free Rh(111) surface. The alloying with Ni makes the assignment of the grey levels much more difficult but it is probably safe to attribute the very dark areas in PEEM to chemisorbed oxygen.

In the Ni coverage range from 0.13 ML to 0.4 ML the boundary excitable/oxygen free shifts very strongly with increasing Ni coverage changing by almost a factor of three. Remarkably, beyond  $\Theta_{\text{Ni}} = 0.4 \text{ ML}$ , a further increase of the Ni coverage has hardly any effect on this boundary. Quite in contrast to the boundary excitable/oxygen free, the boundary oxygen covered/excitable shows only a weak dependence on the Ni coverage over the whole width of the diagram. Only at very high Ni coverages, at about 10 MLs of Ni, the excitability of the system is completely suppressed.

While the boundaries of the excitability range are almost independent of the Ni coverage beyond  $\Theta_{\text{Ni}} = 0.4 \text{ ML}$ , the wave patterns vary quite strongly with the Ni coverage as demonstrated by the PEEM images in Fig. 3. In these experiments we compare the properties of chemical waves keeping the temperature,  $p(\text{O}_2)$ , and  $p(\text{H}_2)$  constant and varying only the

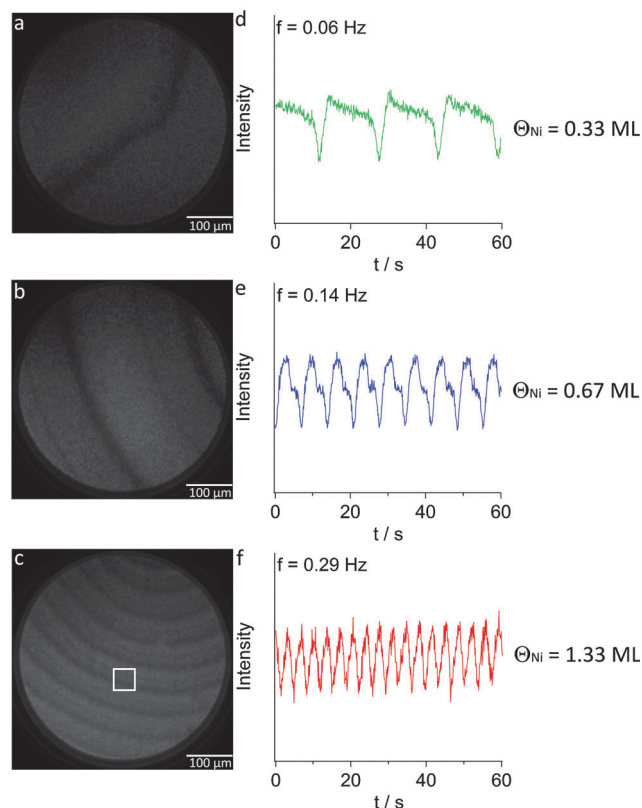


**Fig. 3** Dependence of the chemical waves on the Ni coverage. Shown are PEEM images (a–c) and the local oscillation frequency (d–f) as determined by integrating the PEEM intensity in a small window of  $1000 \mu\text{m}^2$  size indicated in (c). The temperature ( $773 \text{ K}$ ) and the partial pressure of oxygen ( $5.0 \times 10^{-5} \text{ mbar}$ ) were held constant while the nickel coverage and the partial pressure of hydrogen varied as follows: (a + d):  $\Theta_{\text{Ni}} = 0.33 \text{ ML}$ ,  $p(\text{H}_2) = 3.0 \times 10^{-5} \text{ mbar}$  (b + e):  $\Theta_{\text{Ni}} = 0.67 \text{ ML}$ ,  $p(\text{H}_2) = 4.0 \times 10^{-5} \text{ mbar}$  (c + f):  $\Theta_{\text{Ni}} = 1.33 \text{ ML}$ , and  $p(\text{H}_2) = 3.4 \times 10^{-5} \text{ mbar}$ .

Ni coverage. The hydrogen partial pressure is not exactly constant but varies in a range of  $\pm 0.5 \times 10^{-5} \text{ mbar}$  around  $3.5 \times 10^{-5} \text{ mbar}$ . The properties of the chemical waves are only evaluated after having the patterns going for at least one hour. In this way any transient effects are avoided.

With increasing Ni coverage the wavelength of the pulse trains decreases from  $600 \mu\text{m}$  at  $\Theta_{\text{Ni}} = 0.33 \text{ ML}$  to  $60 \mu\text{m}$  at  $\Theta_{\text{Ni}} = 1.33 \text{ ML}$ . Local time series constructed by integrating the PEEM intensity inside a window of  $\sim 1000 \mu\text{m}^2$  size (Fig. 3c) show that the frequency of the local PEEM intensity oscillations increases with increasing Ni coverage. A plot of the local oscillation frequency vs. Ni coverage in Fig. 4 demonstrates a linear relationship over a Ni coverage range from 0.13 ML to 1.3 ML. Quite in contrast to the very strong variation of the oscillation frequency with Ni coverage the propagation velocity varies little as shown in Fig. 4. There is some spread in the velocity between  $15$  and  $35 \mu\text{m s}^{-1}$  but this spread does not seem to exhibit a systematic dependence on the Ni coverage. For explaining the experimental observations a detailed mechanistic model would be required but some of the trends seen in this diagram can nevertheless be explained tentatively. The strong shift of the boundary excitable/oxygen free with increasing Ni coverage between  $\Theta_{\text{Ni}} = 0.13 \text{ ML}$

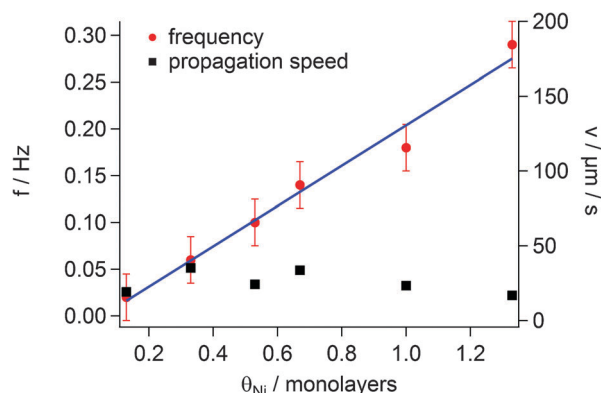


Fig. 4 Dependence of the local oscillation frequency and of the propagation speed of the pulses on the Ni coverage. The  $p, T$ -parameters  $p(\text{O}_2) = 5.0 \times 10^{-5}$  mbar,  $p(\text{H}_2) \sim 3 \times 10^{-5}$  mbar and  $T = 773$  K were held constant and they were chosen such that regular pulse trains can be observed. The error bars reflect the accuracy with which the frequency can be determined from a time series.

and  $\theta_{\text{Ni}} = 0.4$  ML can be attributed to a increasing Ni coverage making the reduction of the oxygen covered state more and more difficult. Chemically, the effect can be traced back to the higher affinity of Ni to oxygen as compared to Rh. What does not fit into this pattern is the monotonous increase of the oscillation frequency with Ni coverage shown in Fig. 4. One should expect that the oscillation frequency slows down with increasing Ni coverage as it becomes more difficult to remove oxygen from the surface.

The behavior of ultrathin Ni layers exposed to oxygen ( $\theta_{\text{Ni}} < 2$  ML) on Rh(111) and on the vicinal surfaces of Rh(111) has been explored in several detailed structural and spectroscopic studies.<sup>12–15</sup> However, in order to construct an excitation mechanism the dynamic behavior of the Rh/Ni/O phases in a reacting environment needs to be known. Such experiments are currently underway.

## Conclusions

The bifurcation diagram of the  $\text{O}_2 + \text{H}_2$  reaction on a Rh(111) surface alloyed with Ni has been determined. A critical Ni coverage  $\theta_{\text{Ni,crit}} = 0.13$  ML is required for obtaining excitable behavior.

In the excitable range one observes regular pulse trains and irregular chemical wave patterns. With increasing Ni coverage the wavelength of the observed pulses decreases while the frequency increases linearly.

## Acknowledgements

The authors are indebted to the Deutsche Forschungsgemeinschaft (DFG) for its financial support.

## References

- 1 J. H. Sinfelt, *Bimetallic catalysts. Discoveries, concepts, and applications*, Wiley, New York, 1983.
- 2 C. Campbell, *Annu. Rev. Phys. Chem.*, 1990, **41**, 775–837.
- 3 J. Rodriguez, *Surf. Sci. Rep.*, 1996, **24**, 223–287.
- 4 A. Christensen, A. V. Ruban, P. Stoltze, K. W. Jacobsen, H. L. Skriver and J. K. Nørskov, *Phys. Rev. B: Condens. Matter Mater. Phys.*, 1997, **56**, 5822–5834.
- 5 J. Greeley, J. K. Nørskov and M. Mavrikakis, *Annu. Rev. Phys. Chem.*, 2002, **53**, 319–348.
- 6 F. Lovis, T. Smolinsky, A. Locatelli, M. Á. Niño and R. Imbihl, *J. Phys. Chem. C*, 2012, **116**, 4083–4090.
- 7 A. Schaak and R. Imbihl, *J. Chem. Phys.*, 2000, **113**, 9822.
- 8 Z. Kurtanek, M. Sheintuch and D. Luss, *Ber. Bunsen. Phys. Chem.*, 1980, **84**, 374–377.
- 9 L. T. Tsitsopoulos and T. T. Tsotsis, *Surf. Sci.*, 1987, **187**, 165–174.
- 10 S. L. Lane and D. Luss, *Phys. Rev. Lett.*, 1993, **70**, 830–832.
- 11 H. H. Rotermund, *Surf. Sci. Rep.*, 1997, **29**, 265–364.
- 12 A. Wander, C. J. Barnes, L. D. Mapledoram and D. A. King, *Surf. Sci.*, 1993, **281**, 42–50.
- 13 T. Franz, J. Zabloudil, F. Mittendorfer, L. Gragnaniello, G. Parteder, F. Allegretti, S. Surnev and F. P. Netzer, *J. Phys. Chem. Lett.*, 2012, **3**, 186–190.
- 14 J. Schoiswohl, F. Mittendorfer, S. Surnev, M. G. Ramsey, J. N. Andersen and F. P. Netzer, *Phys. Rev. Lett.*, 2006, **97**, 126102.
- 15 G. Parteder, F. Allegretti, M. Wagner, M. G. Ramsey, S. Surnev and F. P. Netzer, *J. Phys. Chem. C*, 2008, **112**, 19272–19278.